

High-pressure crystal structure of HgTe-IV

M. I. McMahon, N. G. Wright,* D. R. Allan,† and R. J. Nelmes

Department of Physics and Astronomy, The University of Edinburgh, Mayfield Road, Edinburgh, EH9 3JZ, United Kingdom

(Received 6 July 1995)

The crystal structure of HgTe-IV has been determined using angle-dispersive diffraction techniques, with synchrotron radiation and an image-plate area detector. The structure is not β tin, as previously reported, but is found to be site ordered and orthorhombic with space group $Cmcm$. This is the same structure as has recently been found for CdTe-III/IV and ZnTe-III. However, HgTe exhibits a behavior different from either CdTe or ZnTe, in having a strongly first-order transition from a NaCl phase (HgTe-III) to $Cmcm$. The volume decrease at the transition is 1.2(1)%, and the $Cmcm$ structure just above the transition is strongly distorted from NaCl. Two slightly different, but distinct, configurations of the structure give very similar fits to the diffraction data. Both configurations have significantly different coordination from CdTe-III/IV and ZnTe-III.

I. INTRODUCTION

Among the II-VI semiconductors, the high-pressure behavior of HgTe has attracted the most attention. Bridgman's initial volumetric studies suggested that HgTe undergoes a first-order phase transition at 1.25 GPa with a volume change of $\sim 8.4\%$.¹ This transition was subsequently confirmed by resistivity measurements² and diffraction studies which showed the transition was from the ambient-pressure zincblende structure to the hexagonal cinnabar structure.³ A more detailed analysis of the cinnabar phase, and its pressure dependence, has been made only recently.^{4,5} These reveal that the HgTe cinnabar structure is quite different from that of HgS cinnabar: HgTe cinnabar is 4+2 coordinated,⁴ while HgS cinnabar is 2+4 coordinated.⁶

At higher pressures, resistivity measurements to 20 GPa have revealed two further transitions at 8.4 and ~ 12 GPa.⁷ Initial diffraction measurements reported that these transitions were to a NaCl and an undetermined structure, respectively.⁸ Subsequent studies identified the phase above 12 GPa (HgTe-IV) as having either the β -tin structure⁹ or an orthorhombic structure,^{10,11} related to that observed in some alkali halides and IV-VI compounds. In further work,¹² the latter interpretation was attributed to a mixed phase-III/phase-IV pattern, and the structure of phase IV was revised to a body-centered tetragonal structure—but probably different from β tin in having Hg at (0,0,0) with the Te at $(0, \frac{1}{2}, 0)$ rather than $(0, \frac{1}{2}, \frac{1}{4})$. Huang and Ruoff¹² also reported the existence of a further transition at 38.1 GPa to a phase that may have a distorted CsCl structure.

Recently, as part of a systematic study of the high-pressure behavior of the core II-VI, III-V, and group-IV semiconductors, we have completed detailed studies of ZnTe (Ref. 13) and CdTe,¹⁴ which have revealed that both materials possess a previously unobserved high-pressure orthorhombic structure with space group $Cmcm$. We have already noted¹⁵ that the $Cmcm$ diffraction profiles of CdTe (in phases III and IV),¹⁶ and ZnTe (in phases III), have many similarities with diffraction profiles obtained from HgTe-IV, suggesting that HgTe-IV may, too, have the $Cmcm$ structure. In this paper, we describe our diffraction results on HgTe-IV,

and compare the structure of HgTe-IV with those of CdTe-III/IV and ZnTe-III.

II. EXPERIMENTAL TECHNIQUES

Diffraction data were collected on station 9.1 at the Synchrotron Radiation Source, Daresbury, using angle-dispersive diffraction techniques and an image-plate area detector. The incident wavelength was calibrated at 0.4649(1) Å. In order to determine whether the structure of HgTe-IV is site ordered, we have also performed anomalous dispersion measurements near to both the Te K edge (at 0.3897 Å) and the Hg L_{III} edge (at 1.0094 Å). The two-dimensional powder patterns collected on the image plates were read on a Molecular Dynamics 400A PhosphorImager and then integrated to give conventional one-dimensional diffraction profiles. Details of our experimental setup and pattern integration program have been reported previously.¹⁷

Diacell DXR-4 and Merrill-Bassett diamond-anvil pressure cells were used, with culet diameters of 600 μm . These cells have full conical apertures of 50° and 40° half-angle, respectively. Samples were loaded with a 4:1 mixture of methanol:ethanol as the pressure-transmitting medium, and the pressure was measured using the ruby-fluorescence technique.¹⁸

III. ANALYSIS AND RESULTS

Figure 1 shows a sequence of three integrated profiles obtained from a sample of HgTe as the pressure was increased from 8.4 GPa in the NaCl HgTe-III phase to 18.5 GPa in phase IV. Reflections from the HgTe-IV phase were first observed at 10.2 GPa, ~ 1 GPa lower than previously reported values for the HgTe-III \rightarrow HgTe-IV transition pressure.^{9,12} At 11.5 GPa (Fig. 1), the profile is an approximately 1:2 mixture of the NaCl phase and HgTe-IV: the asterisk marks the remaining (220) reflection of the NaCl phase, and the NaCl (200) reflection can be seen as a shoulder in the part of the 11.5 GPa profile enlarged in the inset. Single-phase patterns of HgTe-IV were obtained at pressures above 13 GPa, and the NaCl (220) reflection can be seen to be completely absent from the 18.5 GPa profile.

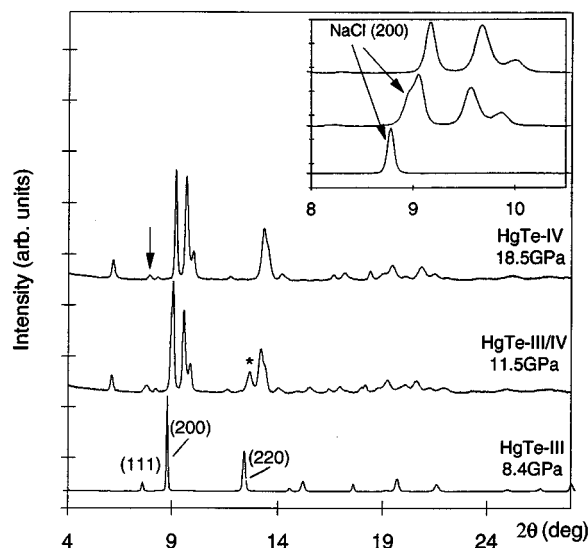


FIG. 1. Integrated profiles obtained from a sample of HgTe in phase III at 8.4 GPa, in a mixture of phases III and IV at 11.5 GPa, and in phase IV at 18.5 GPa. The 2θ range around the position of the NaCl (200) reflection is enlarged in the inset. Marked and labeled reflections are discussed in the text.

The large number of reflections observed in the single-phase HgTe-IV profiles cannot be explained by the β -tin structure or the similar tetragonal structure proposed in Refs. 9 and 12, respectively. However, it was possible to index all the reflections in the HgTe-IV profiles using a C -face-centered orthorhombic cell.^{15,19} Analysis of the systematically absent reflections revealed that, as in CdTe-III/IV and ZnTe-III, the space group of HgTe-IV is $Cmcm$, $C2cm$, or $Cmc2_1$ —the (110) reflection, the observation of which in CdTe-III/IV (Ref. 14) and ZnTe-III (Ref. 13) allowed the space group $Cmca$ to be ruled out, is clearly visible in HgTe-IV at $2\theta \sim 6^\circ$. In order to determine whether the structure of HgTe-IV is site ordered or not, diffraction profiles were collected near to, and far from, the Te K and the Hg L_{III} absorption edges.¹⁹ The difference in scattering power between Hg and Te is increased at the Te edge and (strongly) reduced at the Hg edge. In a site-ordered structure, these changes will particularly affect the relative intensity of weak reflections in which Hg and Te scatter in (or close to) antiphase. Reflections such as the one marked by an arrow in the 18.5 GPa profile were found to become relatively stronger near the Te edge and almost to disappear at the Hg edge. The structure is thus confirmed to be site ordered.

Patterns collected from HgTe-IV were often affected, sometimes severely, by the tendency of this phase to adopt strong, nonaxial, preferred orientation (PO).¹⁹ Samples affected by such PO were easily distinguished by the strong intensity variations around the Debye-Scherrer rings, and, in many cases, the complete absence of reflections with $l \gg h$ and k , such as (002). However, Rietveld refinement was performed only on samples in which there was little or no PO, such as the sample used to obtain the profiles in Fig. 1.

As in ZnTe and CdTe, $Cmcm$ was adopted as the most probable space group for initial refinements. The relative intensities of the (021) and (221) reflections in the HgTe-IV

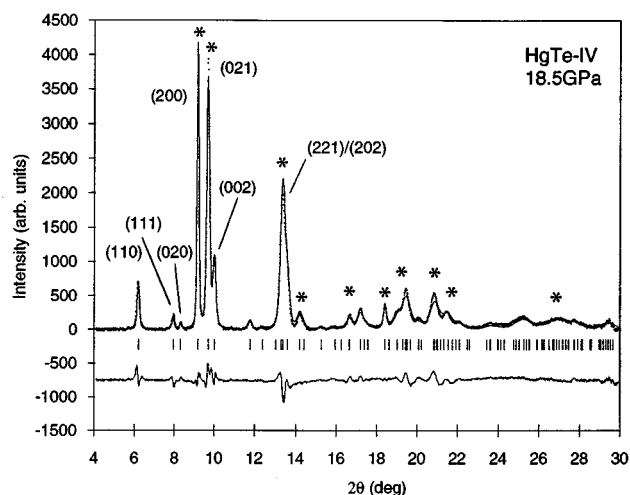


FIG. 2. Rietveld refinement fit to the powder profile of HgTe at 18.5 GPa. The observed data are shown by dots and the fit by a solid line. The tick marks below the profile show the positions of the reflections allowed by the $Cmcm$ space-group symmetry. The difference between the observed and calculated profiles is displayed below the tick marks. The reflections marked with an asterisk correspond to those reported previously in Ref. 12.

profiles collected immediately above the NaCl \rightarrow $Cmcm$ transition suggest that the $Cmcm$ structure is strongly distorted from NaCl. The fit obtained in a Rietveld refinement of the HgTe profile collected at 18.5 GPa, using the $Cmcm$ structure of CdTe at 20 GPa as a starting point, is shown in Fig. 2. The final refined lattice parameters are $a = 5.5626(2)$ Å, $b = 6.1516(5)$ Å, and $c = 5.1050(8)$ Å, and the refined atomic coordinates are Hg (0, y , 0.25) with $y(\text{Hg}) = 0.624(1)$ and Te (0, y , 0.25) with $y(\text{Te}) = 0.152(1)$. Trial refinements were also carried out in the two lower-symmetry space groups $C2cm$ and $Cmc2_1$, but showed no significant evidence of the symmetry of HgTe-IV being lower than $Cmcm$.

The structure thus obtained for HgTe-IV at 18.5 GPa is shown in Fig. 3. As in CdTe and ZnTe, the structure comprises flat NaCl-like layers perpendicular to (001), but with alternate layers displaced ± 0.11 along the y axis. The magnitude of this displacement is larger than that observed in both ZnTe and CdTe, which have y displacements of about ± 0.08 , at 15.7 and 18.6 GPa, respectively. Also, the NaCl-like layers are distorted from true NaCl by (i) the difference in a and b lattice parameters, and (ii) the difference in $y(\text{Hg}) - y(\text{Te})$ (Δy) from 0.5. The magnitudes of a/b and Δy , which are 1.106(1) and 0.472(1), respectively, are to be compared with 1.070(1) and 0.470(4) in CdTe at 18.6 GPa, and 1.112(1) and 0.450(1) in ZnTe at 15.7 GPa.

The coordination of the structure is shown in Fig. 3 and Table I [under $Cmcm(1)$]. The table lists the coordinates of the four Hg and four Te atoms within the unit cell outlined in Fig. 3. The coordinates of atoms 2, 3, and 4 are related to those of atom 1 by symmetry; it is the y coordinates of Hg1 and Te1 that are varied in the structure refinement. There are six different nearest-neighbor contacts, labeled a to f . Like-atom contact distances are shown in italics. As in CdTe, a labels the closest contacts along X ; b and d are, respectively,

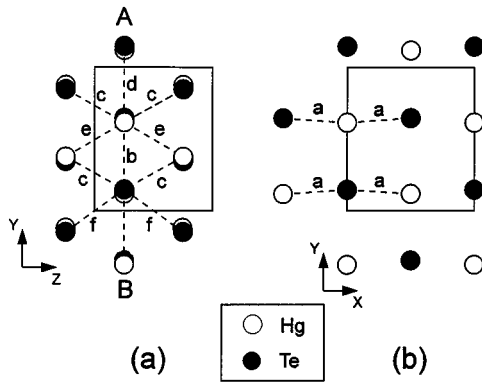


FIG. 3. The $Cmcm$ structure of HgTe-IV at 18.5 GPa. (a) shows a view along the x axis and (b) shows the AB plane in (a) viewed along the z axis. The dashed lines mark the nearest-neighbor contacts around the Hg atom at $(0,0.624,1/4)$ and the Te atom at $(0,0.152,1/4)$. The letters label the six different nearest- and next-nearest-neighbor distances.

the shorter and longer close contacts along Y ; c are the closest unlike-atom contacts between adjacent NaCl-like sheets; and e and f are, respectively, the closest Hg-Hg and Te-Te contacts between adjacent NaCl-like sheets. (See Ref. 20 in relation to the different labeling adopted for ZnTe.) The Hg and Te atoms are both in a quasihexagonal environment, with eight nearest neighbors. The values of the contact distances are spaced in Table I in approximate correspondence with their magnitudes, and it can be seen that the two a , two c , and one b unlike-atom contacts around Hg and Te are all shorter than the two shortest like-atom contacts (e and f , respectively), with one more unlike-atom contact (d) somewhat further away. The closest-neighbor coordination is thus fivefold as found in ZnTe and CdTe, but less clearly so—especially for the Hg atom. In ZnTe and CdTe, the a , b , and c distances are all the same within ~ 0.03 Å, and the other three contacts are 0.3 Å, or more, larger for both the Zn/Cd and the Te atoms.

For the $Cmcm$ structure, it is necessary to consider a second configuration in which the spatial arrangement of atomic sites is similar, but the closest contact between adjacent NaCl-like sheets involves two like rather than unlike atoms.^{13,14} The refined atomic coordinates for this configuration are given in Table I under $Cmcm(2)$. To a first approximation, this structure is related to $Cmcm(1)$ by shifts along y of -0.02 and $+0.02$ for the NaCl-like sheets at $z = \frac{1}{4}$ and $\frac{3}{4}$, respectively. In addition, there is a small change in the difference in $y(\text{Hg}) - y(\text{Te})$, Δy , from 0.5: this changes to 0.478(1), closer to 0.5 than the value of 0.472(1) in $Cmcm(1)$. Though these changes are all quite small, it can be seen in Table I that the coordination of $Cmcm(2)$ is markedly different from $Cmcm(1)$ —particularly for Hg—and the coordination can certainly no longer be described as 5+3.

In both ZnTe and CdTe, it proved possible to discriminate decisively in favor of the $Cmcm(1)$ configuration on the basis of small but significant improvements in the fit compared with that given by $Cmcm(2)$. In CdTe, where the transition from NaCl to $Cmcm$ is continuous, it can additionally be argued that the $Cmcm(1)$ configuration must be correct because a continuous distortion of NaCl cannot reach

TABLE I. Refined atomic coordinates and nearest-neighbor contact distances in two configurations of the $Cmcm$ structure of HgTe at 18.5 GPa. The spacings of the contact distances approximately correspond to their relative magnitudes. Distances shown in italics are between like atoms. In $a(2)$, $c(2)$, etc., the number in parentheses shows the number of a , c , etc., contacts around each atom.

		$Cmcm(1)$		$Cmcm(2)$		
Hg Coordinates	Hg1	0,0.624, $\frac{1}{4}$	Hg1	0,0.606, $\frac{1}{4}$		
	Hg2	0,0.376, $\frac{3}{4}$	Hg2	0,0.394, $\frac{3}{4}$		
	Hg3	$\frac{1}{2}$,0.124, $\frac{1}{4}$	Hg3	$\frac{1}{2}$,0.106, $\frac{1}{4}$		
	Hg4	$\frac{1}{2}$,0.876, $\frac{3}{4}$	Hg4	$\frac{1}{2}$,0.894, $\frac{3}{4}$		
Contacts (Å)	$a(2)$	2.787(1)	$a(2)$	2.785(1)		
	$c(2)$	2.898(4)	$e(2)$	2.865(4)		
	$b(1)$	2.903(9)	$b(1)$	2.939(9)		
	$e(2)$	2.976(4)	$c(2)$	3.033(5)		
	$d(1)$	3.248(9)	$d(1)$	3.213(9)		
	Te Coordinates	Te1	0,0.152, $\frac{1}{4}$	Te1	0,0.128, $\frac{1}{4}$	
		Te2	0,0.848, $\frac{3}{4}$	Te2	0,0.872, $\frac{3}{4}$	
		Te3	$\frac{1}{2}$,0.652, $\frac{1}{4}$	Te3	$\frac{1}{2}$,0.628, $\frac{1}{4}$	
		Te4	$\frac{1}{2}$,0.348, $\frac{3}{4}$	Te4	$\frac{1}{2}$,0.372, $\frac{3}{4}$	
	Contacts (Å)	$a(2)$	2.787(1)	$a(2)$	2.785(1)	
$c(2)$		2.898(4)				
$b(1)$		2.903(9)	$b(1)$	2.939(9)		
			$f(2)$	2.999(5)		
			$c(2)$	3.033(5)		
$f(2)$		3.168(5)				
$d(1)$	3.248(9)	$d(1)$	3.213(9)			

$Cmcm(2)$ until $y(\text{Cd})$ and $y(\text{Te})$ become less than 0.625 and 0.125, respectively—or, more precisely, until $y(\text{Cd})$ becomes less than ~ 0.615 for $\Delta y \sim 0.47$. In the case of HgTe, the $Cmcm(1)$ structure gives the slightly poorer fit, though this can be seen clearly only as a 0.6% decrease in the calculated intensity of the weak (111) reflection (see Fig. 2). Attempts to use anomalous dispersion techniques at the Te K edge and the Hg L_{III} edge to enhance the discrimination between the two configurations also led to (similarly) inconclusive results, still showing a marginally better fit for $Cmcm(2)$. And the strongly first-order nature of the NaCl \rightarrow $Cmcm$ transition prevents the use of any continuity argument.

The diffraction data thus give very small, but consistent, indications—the same in different samples and at the widely varying incident wavelengths used—in favor of $Cmcm(2)$. Comparison with CdTe and ZnTe, and a preference for unlike-atom nearest neighbors, favor $Cmcm(1)$. It does not seem possible to reach a more decisive conclusion with the currently best available powder diffraction data.²¹

The possibly quite different coordination of the $Cmcm$ structure in HgTe may be associated with the strongly first-

order nature of the NaCl→*Cmcm* transition in this case. Unlike in CdTe, the orthorhombic distortion is fully established at the lowest pressure at which the *Cmcm* phase appears. For example, the discontinuous jump in the *a* lattice parameter is evident in the inset to Fig. 1, where the NaCl (200) reflection is seen as a shoulder on the *Cmcm* (200) reflection and clearly displaced from it. Refinements of mixed-phase samples yield a volume change ($\Delta V/V_0$) of 1.2(1)% between the two phases at 11 GPa. The character of the NaCl→*Cmcm* transition is thus quite different from the apparently continuous transition in CdTe. The behavior of HgTe also differs from that of ZnTe. Although the ZnTe-II→ZnTe-III transition is first order, with a volume decrease of 5.7(2)%, the structure of ZnTe-II is cinnabar, which is already a strongly distorted NaCl structure; so it is unsurprising that the *Cmcm* structure immediately above this transition is also well distorted from NaCl.

Finally, we note that all of the observed peaks in the energy-dispersive (ED) diffraction pattern reported by Huang and Ruoff at 17 GPa (see Fig. 2 and Table II of Ref. 12) can be accounted for by a *Cmcm* structure with $a=5.527$ Å, $b=6.109$ Å, and $c=5.061$ Å—as set out in Ref. 22. Their observed reflections constitute the most intense peaks in the HgTe-IV profile, as marked by asterisks in Fig. 2. [The readily detectable *Cmcm* (110) reflection lies under fluorescence lines in the ED pattern of Ref. 12.] We note that all

three lattice parameters are ~0.7% smaller than those observed in the present study at 18.5 GPa, but can offer no explanation for this apparent offset.

In conclusion, we have shown that the structure of HgTe-IV is not, as previously reported, β tin or β -tin-like, but orthorhombic with space group *Cmcm*. This structure accounts for the previously observed diffraction pattern at 17 GPa,¹² and is the same structure as that obtained recently for ZnTe-III and for CdTe-III/IV. HgTe, CdTe, and ZnTe are thus now shown to have a common zinc-blende, cinnabar, NaCl, and then *Cmcm* sequence of phases, except that ZnTe lacks the NaCl phase at ambient temperature. This feature of ZnTe, and the fact that the NaCl→*Cmcm* transition in HgTe is strongly first order, unlike in CdTe, means that the character of the transition to the *Cmcm* phase is markedly different in all three of these II-VI tellurides.

ACKNOWLEDGMENTS

We would like to thank A. A. Neild and G. Bushnell-Wye of the Daresbury Laboratory for their help in preparing the beamline equipment. This work is supported by a grant from the Engineering and Physical Sciences Research Council and by facilities made available by Daresbury Laboratory. Valued assistance with the maintenance and development of pressure cells has been given by D. M. Adams of Diacell Products.

*Present Address: Department of Electrical and Electronic Engineering, University of Newcastle, Newcastle upon Tyne, NE1 7RU, UK.

†Present Address: Bayerisches Geoinstitut, Universität Bayreuth, D-95440 Bayreuth, Germany.

¹P. W. Bridgman, Proc. Am. Acad. Art Sci. **74**, 24 (1940).

²J. Blair and A. Smith, Phys. Rev. Lett. **7**, 124 (1961).

³A. N. Mariano and E. P. Warekois, Science **142**, 672 (1963).

⁴N. G. Wright, M. I. McMahon, R. J. Nelmes, and A. San Miguel, Phys. Rev. B **48**, 13 111 (1993).

⁵A. San Miguel, N. G. Wright, M. I. McMahon, and R. J. Nelmes, Phys. Rev. B **51**, 8731 (1995).

⁶K. Aurivillius, Acta Chem. Scand. **4**, 1413 (1950).

⁷A. Ohtani, T. Seike, M. Motobayashi, and A. Onodera, J. Phys. Chem. Solids **43**, 627 (1982).

⁸A. Onodera, A. Ohtani, M. Motobayashi, T. Seike, O. Shimomura, and O. Fukunaga, in *Proceedings of the 8th AIRAPT Conference, Uppsala*, edited by C. M. Backman, T. Johannison, and L. Tengner (Aritektopia, Uppsala, 1982), Vol. 1, p. 321.

⁹A. Werner, H. D. Hochheimer, and K. Strössner, Phys. Rev. B **28**, 3330 (1983).

¹⁰T. Huang and A. L. Ruoff, Phys. Status Solidi A **77**, K193 (1983).

¹¹T. Huang and A. L. Ruoff, in *Proceedings of 9th AIRAPT Conference, High Pressure Science and Technology* (North Holland, New York, 1994), Pt. 3, Vol. 22, p. 37.

¹²T. Huang and A. L. Ruoff, Phys. Rev. B **31**, 5976 (1985).

¹³R. J. Nelmes, M. I. McMahon, N. G. Wright, and D. R. Allan, Phys. Rev. Lett. **73**, 1805 (1994).

¹⁴R. J. Nelmes, M. I. McMahon, N. G. Wright, and D. R. Allan,

Phys. Rev. B **51**, 15 723 (1995).

¹⁵M. I. McMahon, R. J. Nelmes, N. G. Wright, and D. R. Allan, in *Proceedings of the Joint AIRAPT/APS Topical Conference on High Pressure Science and Technology*, Colorado Springs 1993, edited by S. Schmidt [American Institute of Physics, New York (1994)], p. 633.

¹⁶CdTe-III and CdTe-IV have been shown in Ref. 14 to be one and the same phase, denoted CdTe-III/IV in this paper.

¹⁷R. J. Nelmes and M. I. McMahon, J. Synch. Radiat. **1**, 69 (1994), and references cited therein.

¹⁸H. K. Mao, P. M. Bell, J. W. Shaner, and D. J. Steinberg, J. Appl. Phys. **49**, 3276 (1978).

¹⁹N. G. Wright, Ph.D. thesis, University of Edinburgh, 1994.

²⁰A different, less general, labeling was adopted in ZnTe (Ref. 13) in which the contact distances were labeled *a* to *f* in the sequence of increasing magnitude. For comparison with HgTe and CdTe, the ZnTe contacts *a* to *f* need to be relabeled *b*, *c*, *a*, *e*, *d*, and *f*.

²¹This type of ambiguity in structures with variable coordinates may be expected to arise in powder diffraction (as against single-crystal diffraction) in general, and not as a peculiarity of high-pressure studies. However, increased peak overlap in powder profiles due to pressure broadening will make the problem more likely to occur at high pressures.

²²Huang and Ruoff (Ref. 12) gave the measured *d* spacings of ten observed peaks. They index on the *Cmcm* structure as follows: 2.762 Å (200), 2.618 Å (021), 1.896 Å (221), 1.788 Å (131), 1.526 Å (040), 1.385 Å (400), 1.314 Å (331/042), 1.219 Å (313), 1.184 Å (242), and 0.948 Å (442).